

Bis(morpholino-1,3,5-triazine) Derivatives: Potent Adenosine 5'-Triphosphate Competitive Phosphatidylinositol-3-kinase/Mammalian Target of Rapamycin Inhibitors: Discovery of Compound 26 (PKI-587), a Highly Efficacious Dual Inhibitor

Aranapakam M. Venkatesan,^{*,†} Christoph M. Dehnhardt,[†] Efren Delos Santos,[†] Zecheng Chen,[†] Osvaldo Dos Santos,[†] Semiramis Ayrar-Kaloustian,[†] Gulnaz Khafizova,[†] Natasja Brooijmans,[†] Robert Mallon,[‡] Irwin Hollander,[‡] Larry Feldberg,[‡] Judy Lucas,[‡] Ker Yu,[‡] James Gibbons,[‡] Robert T. Abraham,[‡] Inder Chaudhary,[§] and Tarek S. Mansour[†]

[†]Chemical Sciences, [‡]Oncology, and [§]Drug Metabolism, Wyeth Research, 401 N. Middletown Road, Pearl River, New York 10965

Received December 11, 2009

The PI3K/Akt signaling pathway is a key pathway in cell proliferation, growth, survival, protein synthesis, and glucose metabolism. It has been recognized recently that inhibiting this pathway might provide a viable therapy for cancer. A series of bis(morpholino-1,3,5-triazine) derivatives were prepared and optimized to provide the highly efficacious PI3K/mTOR inhibitor 1-(4-{[4-(dimethylamino)piperidin-1-yl]carbonyl}phenyl)-3-[4-(4,6-dimorpholin-4-yl-1,3,5-triazin-2-yl)phenyl]urea **26** (PKI-587). Compound **26** has shown excellent activity in vitro and in vivo, with antitumor efficacy in both subcutaneous and orthotopic xenograft tumor models when administered intravenously. The structure–activity relationships and the in vitro and in vivo activity of analogues in this series are described.

Introduction

Phosphatidylinositol-3-kinases (PI3Ks^a) are lipid kinases that phosphorylate phosphatidylinositol diphosphate (PIP2) to its corresponding phosphatidylinositol triphosphate (PIP3). It has been recognized recently that the PI3K/Akt signaling pathway is a key pathway in cell proliferation, growth, survival, protein synthesis, and glucose metabolism.^{1–6} The product of PI3K activity, namely, PIP3, acts as a second messenger responsible for the activation of the downstream kinase Akt.¹ PI3Ks are categorized as class IA, class IB, class II, and class III enzymes, based on sequence homology and substrate preferences. The PI3K related kinases (PIKKs) include mTOR, ATR, ATM, SMG1, and DNA-PK. PIKKs share a conserved kinase domain with PI3Ks and regulate cellular response to nutrient levels and environmental stress. The class IA subgroup consists of PI3K α , PI3K β , and PI3K δ isoforms. Among these three isoforms, the gene encoding the PI3K α subunit, PIK3CA, is mutated and/or overexpressed in breast, ovarian, colorectal, brain (glioblastoma), and gastric cancers.^{6,9–11} Additionally, the PIP3 lipid phosphatase, phosphatase and tensin homologue deleted on chromosome ten (PTEN), is frequently inactivated in numerous late stage tumors, causing elevated

levels of PIP3 with consequent deregulation of the PI3K/Akt pathway signaling.^{1–6} This also contributes to oncogenesis.^{7,8,12} Therefore, inhibiting PI3K α is an attractive strategy for cancer therapy. Furthermore, it has been demonstrated that the PI3K pathway is paradoxically activated following selective mTOR inhibition, thus providing a compelling rationale for developing dual PI3K/mTOR kinase inhibitors.^{13,14}

Toward this end, several pharmaceutical companies and academic institutions have been concentrating their efforts on the development of small molecule PI3K/mTOR inhibitors.^{2,15–17} Among the various small molecule inhibitors, BEZ-235 **1** (Figure 1) is the most advanced clinical candidate.^{19a,b} It inhibits PI3K and mTOR in an ATP-competitive manner. This compound is also reported to inhibit cancer cell proliferation, causing cell cycle arrest at the G1 phase.^{19a,b} Another compound that inhibits all class I PI3K isoforms, but with significantly lower potency against mTOR, is **2** GDC-0941.¹⁸ This compound was reported by Genentech and has entered phase I clinical studies. Another pan PI3K inhibitor that has gone into the clinic is Semafore compound, SF1126.²⁰ Highly selective mTOR inhibitors based on a pyrazolopyrimidine scaffold such as **3a** were reported by Zask et al.^{21a,b} and recently entered clinical development. We also recently described a dual PI3K/mTOR inhibitor **3** (PKI-402) based on a triazolopyrimidine scaffold that has potent in vivo efficacy.^{21c}

In the present article, we describe the design, synthesis, and identification of a highly potent bis(morpholino-1,3,5-triazine) derivative **26** (PKI-587) as a PI3K/mTOR inhibitor. Compound **26** decreases cell survival and proliferation and increases apoptosis in both in vitro and in vivo models. It shows compelling antitumor efficacy in subcutaneous and orthotopic human xenograft tumor models when administered intravenously (iv) as a single agent.

*To whom correspondence should be addressed. Phone: (845) 602-4023. Fax (845) 602-5561. E-mail: venkata@wyeth.com or venkata699@gmail.com.

^a Abbreviations: PI3K, phosphoinositide 3-kinase; mTOR, mammalian target of rapamycin; Akt, protein kinase B; PIP2, phosphatidylinositol bisphosphate(4,5); PIP3, phosphatidylinositol triphosphate(3,4,5); PTEN, phosphatase and tensin homologue; RTK, receptor tyrosine kinase; PH, pleckstrin homology; mTORC1, mammalian target of rapamycin complex 1; mTORC2, mammalian target of rapamycin complex 2; PDK1, 3-phosphoinositide-dependent kinase 1; S, serine; T, threonine; ATP, adenosine 5'-triphosphate; Her2+, human epidermal growth factor receptor 2+; ELISA, enzyme-linked immunosorbent assay; DELFIA, dissociation-enhanced lanthanide fluorescent.

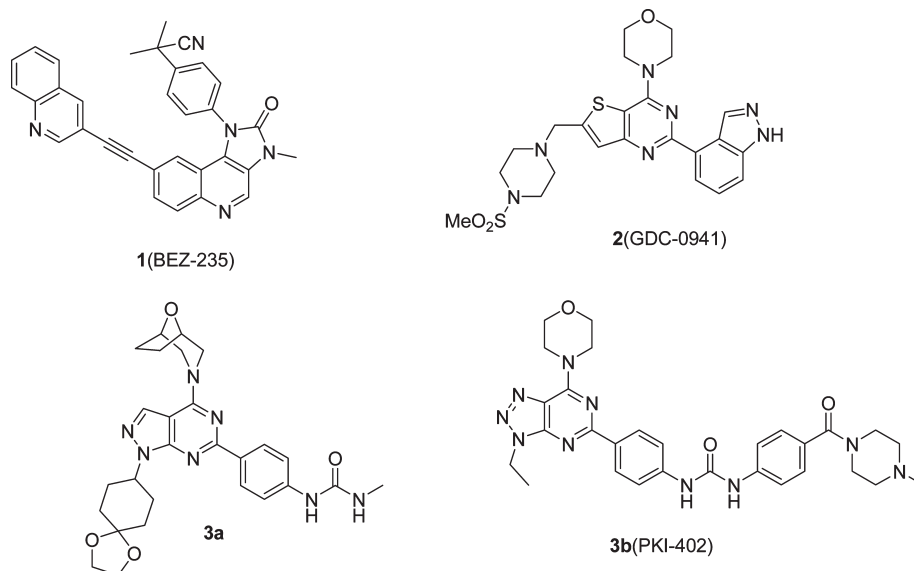


Figure 1. Previously known phosphatidylinositol-3-kinase inhibitors and selective mammalian target of rapamycin inhibitor.

Chemistry

The 2,4-bismorpholino-1,3,4-triazine derivatives **8–30**, which are exemplified in the present article, were prepared starting from the commercially available cyanuric chloride **4**, as outlined in Scheme 1. Initially the two chlorines in cyanuric chloride **4** were replaced with 2 equiv of morpholine **5** in the presence of triethylamine at 0 °C to yield **6** in almost quantitative yield. The third chlorine in compound **6** was displaced by a 4-aminophenyl moiety using Suzuki coupling reaction with 4-aminophenylboronic acid pinacol ester to yield **7**. Compound **7** was reacted with various alkyl and aryl isocyanates to yield **8–14**, **17**, **18**, and **21**. Alternatively, urea derivatives **15**, **16**, **19**, and **20** were obtained by reacting the intermediate **7** with triphosgene/triethylamine and the corresponding amines. In order to introduce amides bearing water solubilizing amine functionality, intermediate **7** was reacted with methyl 4-isocyanatobenzoate in dichloromethane at room temperature to give **21** in good yield. The ester group was hydrolyzed with 5 N NaOH in tetrahydrofuran/methanol at reflux temperature to yield **22**. The acid derivative **22** was reacted with different amines in the presence of HOBt/EDCI and triethylamine at room temperature. The final products were purified either by flash column silica gel column chromatography or by preparative HPLC. All analogues **8–30** obtained by the above-mentioned route were analyzed for purity by analytical HPLC on a prodigy ODS3 column (150 mm × 4.6 mm) using acetonitrile/water mixture. The purity of the newly synthesized compounds was analyzed at 210–370 nm.

Results and Discussion

Final compounds **8–30** were tested *in vitro* against PI3K α , PI3K γ , and mTOR. The IC₅₀ values against PI3K α and PI3K γ enzymes were determined using a fluorescence polarization format assay.²² The corresponding mTOR inhibition for the newly synthesized compounds was determined using a DELFIA format ELISA.²³ PI3K α , PI3K γ , and mTOR as well as the cell proliferation (3 days growth inhibition) assay²⁴ IC₅₀ values in MDA-361 (breast, PI3K mutant [E545K]/Her2+) and PC3MM2 (prostate, PTEN deletion) human tumor cell lines are shown in Table 1. The solubility (at pH 7.4), PAMPA

permeability, and clogP data for analogues **8–30** are also listed in Table 1.

Several morpholine bearing fused pyrimidines such as imidazolopyrimidines,²⁵ pyrrolopyrimidines,²⁶ and triazolopyrimidines^{21c} have been reported by us previously as PI3K/mTOR dual inhibitors. In all these scaffolds, the morpholine oxygen formed a pivotal hinge region hydrogen bond interaction with Val851 of the PI3K α catalytic domain^{18,21a–c} but also presented a metabolic liability via oxidation α to the morpholine ring oxygen, causing loss of potency. Many potent PI3K enzyme inhibitors based on the above-mentioned scaffolds failed to show antitumor efficacy in *in vivo* models. The most advanced compound **3** showed good efficacy in MDA-361 xenograft model. However, advanced studies with **3** were halted because of its poor solubility.

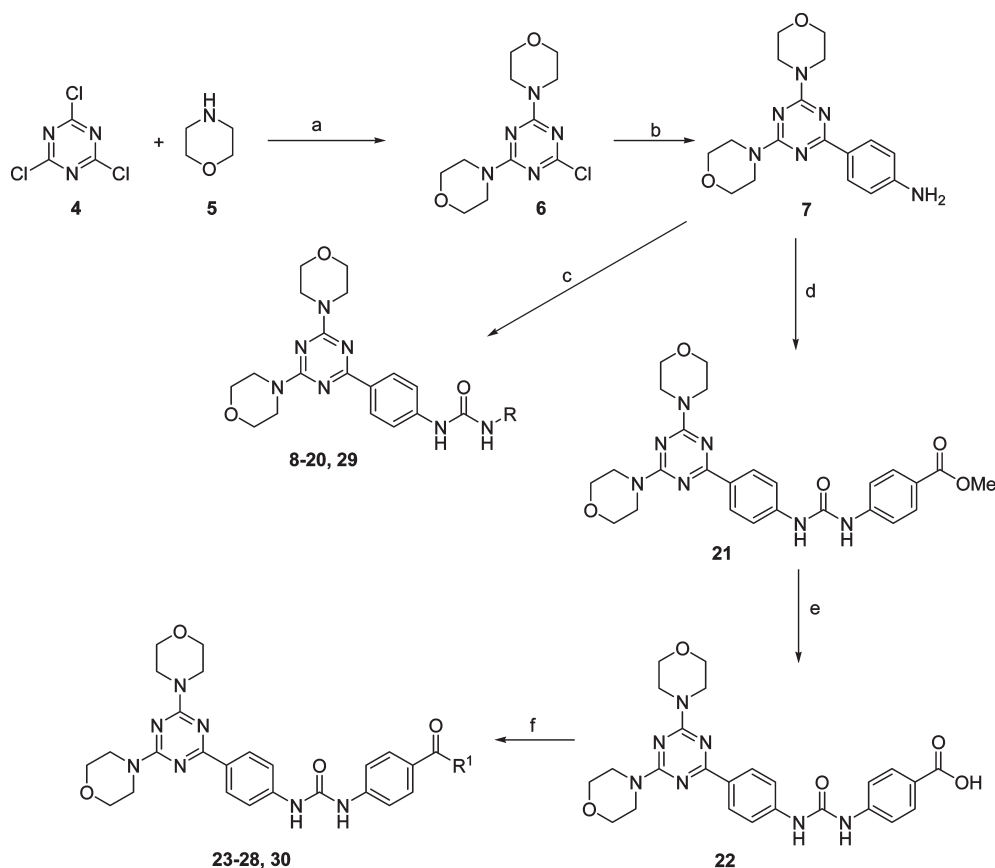
Bearing these facts in mind, we decided to probe the other scaffolds that resemble a pyrimidine core but have lower clogP values than the triazolopyrimidine core in PKI-402. Among the various heterocycles we synthesized, the 1,3,5-triazine scaffold¹⁷ was very attractive for the following reasons:

(1) 1,3,5-Triazine is a monocyclic, symmetrical molecule similar to the pyrimidine core with two nitrogens in the 1,3-positions, and it has been used as a kinase inhibitor scaffold.¹⁷ Hence, we envisaged that 1,3,5-triazine could mimic the pyrimidine scaffold and allow us to position the critical substituents observed in our earlier series for optimum interaction with the binding site of PI3K α .

(2) The presence of three nitrogens in the 1,3,5-triazine core can inherently impart polarity to the whole molecule, and the clogP values of the designed compounds can be about 2 or lower.

(3) We also envisioned also that a bismorpholino-1,3,5-triazine scaffold would have an advantage under conditions where one morpholine gets metabolically oxidized, still leaving another morpholine to make the vital hinge region H bond interaction in the PI3K catalytic domain.

However, we were aware that these modifications can solve the clogP problem, and to an extent, the morpholine metabolic liability might not address permeability and the microsomal stability problems. In order to explore the above-mentioned points, compound **8** was designed and modeled in the PI3K γ homology model (Figure 2). The structural

Scheme 1. General Methods To Prepare **8–30**

Reagents and conditions; (a) Et₃N (5 eq), acetone, crushed ice, -20 °C to 0 °C; (b) 4-Aminophenylboronic acid, pinacol ester (1.2 eq), Pd(Ph₃P)₄ (5 mol%), DME, 2M Na₂CO₃, reflux, 8 h; (c) RNCO, CH₂Cl₂, RT, 4 to 6 h or Triphosgene (0.6 eq), Et₃N (3 eq), Amines (3–5 eq); (d) Methyl-4-isocyanatobenzoate (1.1 eq), CH₂Cl₂, RT; (e) 5N NaOH (3 eq), MeOH, THF, 70 °C, 12h; (f) Amines (2 eq), HOBT (1.5 eq), EDCI (1.5 eq), Et₃N (2 eq), THF, RT, 12 h

| | |
|---|--|
| 8 , R = Phenyl | 17 , R = 2-Thienyl |
| 9 , R = Ethyl | 18 , R = 3-Pyridyl |
| 10 , R = Methyl | 19 , R = 4-Pyridyl |
| 11 , R = 4F-phenyl | 20 , R = 5-Pyridazinyl |
| 12 , R = 4Me-phenyl | 23 , R ¹ = -NHMe |
| 13 , R = 4Cl-phenyl | 24 , R ¹ = -NH-(CH ₂) ₂ -NMe ₂ |
| 14 , R = 2,4difluoro phenyl | 25 , R ¹ = 4-Methylpiperazine |
| 15 , R = 4-CH ₂ OH phenyl | 26 (PKI-587), R ¹ = 4-N(Me) ₂ -piperidine |
| 16 , R = 4-CH ₂ CH ₂ OH phenyl | 27 , R ¹ = 4-Pyrrolidino-piperidine |

| |
|---|
| 28 , R ¹ = 4-Piperidino-piperidine |
| 29 , R = -4-Piperidine |
| 30 , R ¹ = -N(Me)-(CH ₂) ₂ -NMe ₂ |

similarity of the ATP-binding sites of PI3K α and PI3K γ isoforms enabled a homology model to be built based on an in-house X-ray crystal structure of PI3K γ in complex with a related compound (3IBE.pdb).^{21a} Overall sequence similarity between PI3K α and PI3K γ is 43% in the kinase catalytic domain; however, the ATP-binding site is significantly more conserved with 81% of the residues being identical. As indicated in Figure 2, compound **8** docked in the homology model forms the critical hinge region hydrogen-bond to Val851 through a morpholine oxygen. The urea forms two hydrogen-bonding interactions to Asp810 through both urea-NH groups and one to the catalytic lysine (Lys802) through the urea carbonyl group. Hence, compound **8** was prepared as depicted in Scheme 1. As can be seen from Table 1, compound **8** was found to have potent PI3K α , PI3K γ , and mTOR inhibitory activity but only moderate potency in MDA-361 and PC3MM2 cell proliferation assays.

This was attributed to the poor solubility and permeability of compound **8**.

However, this initial enzyme potency result encouraged us to probe the structure–activity relationship more systematically to further optimize the cellular potency. There was an observed drop in the potency against PI3K α and PI3K γ when the phenyl group in compound **8** was replaced with alkyl groups such as methyl **10**, ethyl **9**, or saturated heterocyclyl **29**. However, the corresponding mTOR activity was not affected. The structural basis for the observed difference in PI3K α / γ and mTOR activity for compounds **9**, **10**, and **29** is not entirely clear because of a lack of detailed structural information on the mTOR enzyme (Figure 3). However, three residue differences are observed in the loop that forms the top of the binding site around the urea substituents. Asp805 in PI3K α is a glutamic acid in mTOR, and this residue plays a critical role in stabilizing the catalytic lysine (Lys802 in PI3K α ,

Table 1. In Vitro, Microsomal Stability, Solubility, and clogP Data for Analogues **8**–**30**^a

| compd | IC ₅₀ (nM) | | | | | clogP | sol. ^b at pH 7.4 | PAMPA at pH 7.4 |
|-----------|-----------------------|----------------|-------|---------|---------|-------|-----------------------------|-----------------|
| | PI3K- α | PI3K- γ | mTOR | MDA-361 | PC3-MM2 | | | |
| 8 | 3.0 | 27.0 | 3.9 | 56 | 107 | 2.5 | 0.0 | 0.2 |
| 9 | 247.5 | 814.5 | 10.0 | NT | NT | 1.2 | 1.0 | 0.7 |
| 10 | 350.0 | 789.0 | 11.3 | NT | NT | NA | NT | NT |
| 11 | 6.5 | 52.5 | 3.9 | 118.0 | 193.0 | 2.8 | 0.0 | 1.0 |
| 12 | 16.5 | 438.0 | 6.3 | 200.0 | 364.0 | 3.0 | 0.0 | 5.6 |
| 13 | 19.5 | 219.5 | 6.7 | 407.0 | 293.0 | 3.4 | 1.0 | 0.0 |
| 14 | 60.5 | 528.0 | 9.3 | 794.0 | 5630.5 | 2.5 | 1.0 | 0.0 |
| 15 | 1.0 | 14.5 | 1.9 | 30.0 | 30.0 | 1.5 | 0.0 | 0.2 |
| 16 | 1.5 | 21.5 | 1.8 | 36.0 | 39.0 | 1.7 | 0.0 | 0.0 |
| 17 | 2.0 | 23.0 | 1.7 | NT | 218 | 2.2 | 2.0 | 2.4 |
| 18 | 1.7 | 34.0 | 1.2 | NT | 92 | 1.8 | 0.0 | 0.5 |
| 19 | 3.0 | 28.5 | 1.2 | 45.0 | 43.0 | 1.8 | 0.0 | 1.4 |
| 20 | 11.0 | 65.0 | 2.3 | 38.0 | 21.0 | 1.0 | 1.0 | NT |
| 21 | 12.5 | 85.0 | 2.5 | 115.0 | 45.0 | 2.9 | 1.0 | 0.6 |
| 22 | 6.0 | 48.5 | 1.5 | 816.0 | 28.0 | 2.4 | 52.0 | 0.0 |
| 23 | 1.5 | 20.0 | 0.7 | 19.0 | 24.0 | 1.4 | 1.0 | NT |
| 24 | 0.4 | 8.0 | 0.5 | 3.0 | 11.0 | 1.8 | 7.0 | 0.1 |
| 25 | 0.5 | 9.0 | 1.4 | 10.0 | 13.0 | 2.1 | 0.0 | 0.0 |
| 26 | 0.4 | 5.4 | 1.6 | 4.0 | 13.1 | 1.2 | 14.0 | 0.1 |
| 27 | 0.7 | 10.0 | 0.8 | 3.0 | 8.3 | 2.0 | 33.5 | NT |
| 28 | 0.6 | 10.0 | 0.7 | 3.0 | 7.0 | 2.5 | 31.0 | NT |
| 29 | 1521.0 | 7470.0 | 460.0 | NT | NT | 1.0 | 100.0 | 0.010 |
| 30 | 0.4 | 9.0 | 0.6 | 9.8 | 18.3 | 2.0 | 9.0 | 0.030 |

^aNT = not tested. PAMPA = permeability $Pe \times 10^{-6}$ cm/s. ^bSolubility is in μ g/mL.

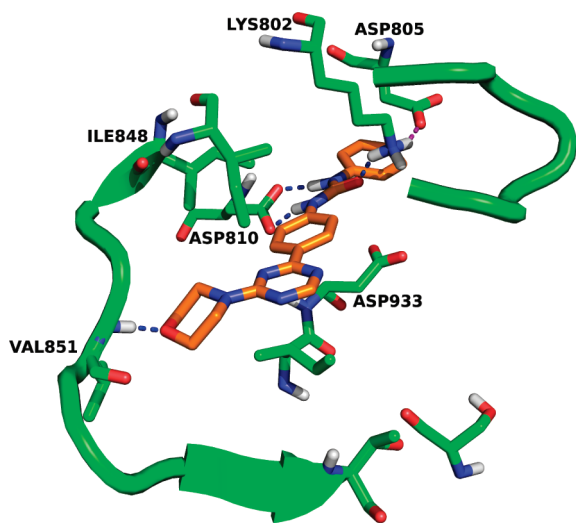


Figure 2. Docking of compound **8** in PI3K γ homology model. Hydrogen bonds are shown by blue dashes. The morpholine forms a hydrogen bond to the hinge region Val851. The urea forms three hydrogen bonds to Asp810 and Lys802. The critical salt bridge between the catalytic Lys802 and Asp805 is shown in purple.

Lys2187 in mTOR) through the formation of a salt bridge. Substituted ureas of this type result in a concerted motion of the catalytic lysine and the aspartic/glutamic acid,^{21a,b} and it is possible that mTOR with the longer side chain in the glutamic acid, compared to the aspartic acid in PI3K α , undergoes this motion more easily. The second noted residue difference in this area is the different positioning of glycine. In PI3K α , a glycine (Gly804) is directly adjacent to the aspartic acid involved in the salt bridge, whereas in mTOR, a histidine (His2189) separates the glutamic acid from the glycine (Gly2188). Again, it is possible that the different position of the glycine allows the mTOR loop to accommodate the hydrophobic groups coming off the urea more easily. Substitution

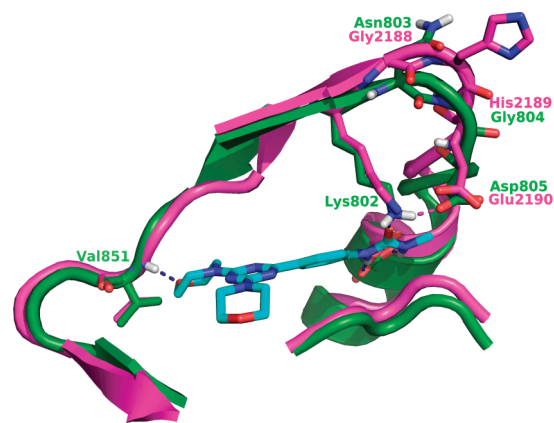


Figure 3. Detailed of interactions of compound **9** with PI3K α and mTOR: overlay of the homology models of PI3K α (green ribbons and carbons) and mTOR (magenta ribbons and carbons) with the predicted binding mode of compound **9**. Conserved residues are Val851 (Val2240 in mTOR) and Lys802 (Lys2187) and are therefore only labeled. Several residue differences near the urea-R groups (in this case R = CH₃) are Asp805-Glu2190, Gly804-His2189, and Asn803-Gly2188.

of the phenyl group in compound **8** with 4-fluoro **11**, 4-methyl **12**, 4-chloro **13**, and 2,4-difluorophenyl **14** led to compounds with moderate PI3K α , PI3K γ , and mTOR potency. It can also be noted from Table 1 that substitution of the phenyl group with a lipophilic group (examples **11**, **12**, **13**, and **14**) led to a decrease in the potency against PI3K α . However, all these compounds, with the exception of **29**, had excellent potency against mTOR. It appears from the different examples that PI3K α potency is favored if the R group is an aryl substituent. Molecular modeling using the PI3K γ homology model revealed that the substituents on the R groups are solvent exposed (Figure 4). Hence, compounds **15** and **16**, bearing polar entities such as $-\text{CH}_2\text{OH}$ and $-\text{CH}_2\text{CH}_2\text{OH}$ were prepared. This modification led to improvement in both enzyme and cellular potencies. This could

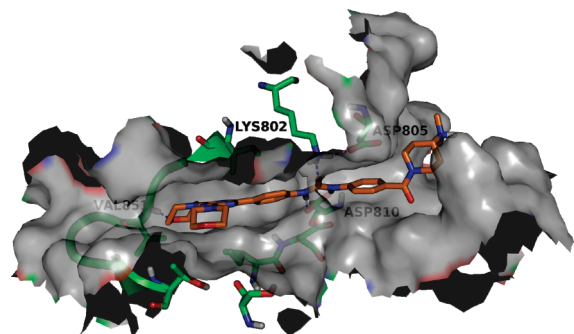


Figure 4. Surface representation of the ATP binding site around **26**, illustrating that substitutions coming off the urea extend into the solvent.

Table 2. IC₅₀ Values against Various PI3K Isoforms and Mutants

| IC ₅₀ (nM) | isoforms | | | | |
|-----------------------|--------------|---------------|---------------|--------|-------|
| | PI3K β | PI3K γ | PI3K δ | H1047R | E545K |
| IC ₅₀ (nM) | 6 | 8 | 6 | 0.6 | 0.6 |

be due to their marginally improved permeability. The PAMPA permeability for compound **15** is 0.18×10^{-6} cm/s, and the Caco2 data for compound **16** is 2.9 (A > B) and 7.2 (B > A). Compounds **15** and **16** had poor human and nude mouse microsomal stabilities, which precluded them from further investigation. Heterocycles **18**, **19**, and **20** containing polar nitrogen also gave potent compounds with slightly increased human and nude mouse microsomal stabilities. However, these analogues did not have a good solubility profile at pH 7.4. Hence, compounds such as **24–30** bearing a basic amine moiety were prepared. As can be seen from Table 1, except for compound **29**, compounds bearing a basic amine moiety with an amide linkage exhibited excellent enzyme and cell potencies. These analogues also had good microsomal stability in all three species and exhibited good to moderate solubility. This dramatic boost in the PI3K α enzyme potency by the amide substituent is not very well understood and may be due to an increased hydrogen bond accepting ability of the overall molecule. On the basis of enhanced potency, solubility, microsomal stability, and lack of Cyp inhibition, compound **26** was chosen for further in vitro and in vivo evaluations. Compound **26** was evaluated for its potency against class I PI3Ks (i.e., the β , γ , and δ isoforms) and the most frequently occurring mutant forms of PI3K α , notably the H1047R and E545K. The IC₅₀ values are shown in Table 2. These results show that compound **26** is a pan-PI3K/mTOR inhibitor, with equivalent potency against mTOR (IC₅₀ = 1.4 nM, Table 1). This compound was also evaluated against a panel of 236 other human protein kinases at 10 μ M, and it was found to be highly selective for PI3K and mTOR.

In vitro, compound **26** showed good potency in cell growth inhibition assays using MDA-361 and PC3-MM2 cell lines. Tumor cell growth inhibition by **26** correlated with suppression of phosphorylation of PI3K/mTOR signaling pathway proteins in MDA-361 tumor cells (Figure 5). Compound **26** prevented the phosphorylation of Akt (pAkt) at threonine 308 (T308; IC₅₀ = 8 nM) (phosphoblot IC₅₀ values were determined by densitometric scans of Western blots) and induced cleaved PARP at 30 nM. Cleaved PARP is a marker for cells undergoing apoptosis. Full activation of Akt kinase occurs when the mTOR containing mammalian target of rapamycin 2 (TORC2) protein complex phosphorylates Akt at serine

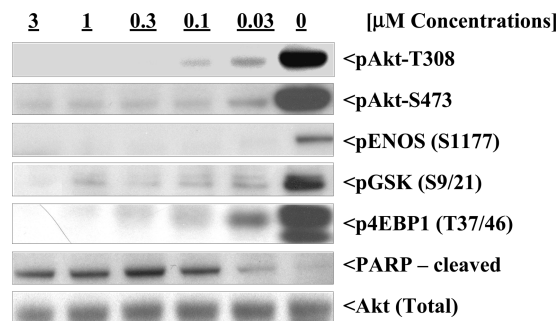


Figure 5. In vitro phosphoblot studies. MDA-361 tumor line was exposed to **26** for 4 h.

473 (S473). Figure 5 also shows potent (IC₅₀ < 10 nM) suppression of Akt phosphorylation at S473 by **26**. Phosphorylation of Akt kinase effector proteins GSK3 kinase, endothelial nitric oxide synthase (ENOS), and prolinerich Akt substrate (PRAS 40) was also suppressed by **26** at concentrations less than 30 nM. The inhibition of mTOR containing TORC1 kinase activity by **26** was demonstrated by suppression of p70S6K and 4EBP1 phosphorylation at concentrations less than 30 nM by **26**. Compound **26** did not affect the overall Akt content in MDA-361 cells at concentrations tested (Figure 5), indicating pAkt suppression was not an artifact of compound cytotoxicity.

Initial blood level studies in female nude mice were done with compounds **24**, **25**, and **26** via both oral (po) and iv routes of administration. None of these three analogues had oral exposure in nude mice. However, when **26** was administered to nude mice at 25 mg/kg iv (in 5% dextrose [D5/W], 0.3% lactic acid, pH 3.5), low plasma clearance (7 (mL/min)/kg) compared to liver blood flow (90 (mL/min)/kg), high volume of distribution (7.2 L/kg) compared to plasma volume (0.7 L/kg), and long half-life, (14.4 h) were observed (Table 3). Low clearance indicated minimal metabolism, and high volume of distribution was suggestive of extensive tissue distribution in nude mice. When compound **26** was administered iv (single dose) at 25 mg/kg, it suppressed pAkt (T308 and S473) for up to 36 h and induced cleaved PARP up to 18 h in MDA-361 tumors staged in nude mice (Figure 6).

Compound **26** exhibiting potent antitumor efficacy against MDA-361 tumors is also demonstrated in Figure 7. Compound **26** administered iv at 20 mg/kg on an intermittent regimen (days 1, 5, 9) caused regression of large staged (~900 mm³) tumors. This effect was more pronounced than that observed for paclitaxel (Taxol) given at 60 mg/kg (single dose, ip). In subsequent in vivo studies the minimum efficacious dose (MED) of **26** was determined to be 3 mg/kg against MDA-361 tumors and maximum tolerated single dose (MTD) was determined to be 30 mg/kg.

Potent antitumor activity of compound **26** was also demonstrated in an orthotopic version of the H1975 (non-small-cell lung carcinoma, mutant EGFR [L858R, T790M]) xenograft model (Figure 8). H1975 cells were injected into the pleural cavity of nude mice, and the animals were treated with **26** once weekly at 25 mg/kg for 7 weeks. As can be seen from Figure 8, all of the untreated control animals were dead by day 50, compared to 90% survival in the group treated with **26**.

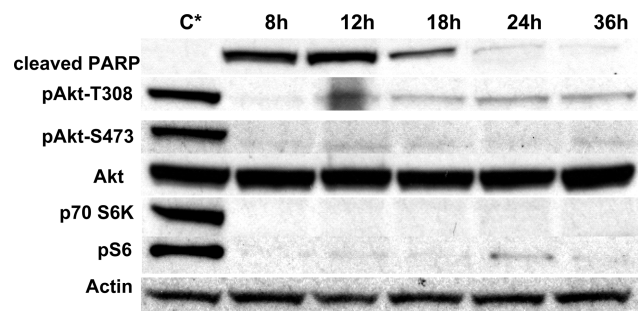
Conclusion

We have shown that bis(morpholinotriazine) compounds bearing bisarylureas are potent dual PI3K/mTOR inhibitors.

Table 3. Pharmacokinetic Parameters of Compound **26** after a Single 25 mg/kg iv Dose in Female Nude Mice^a

| C_0 (ng/mL) | $T_{1/2}$ (h) | AUC_{last} (h·ng/mL) | AUC_{0-inf} (h·ng/mL) | Cl_p ((mL/min)/kg) | V_{ss} (L/kg) | MRT (h) |
|---------------|---------------|------------------------|-------------------------|----------------------|-----------------|---------|
| 48523 | 14.4 | 42593 | 57927 | 7 | 7.2 | 16.7 |

^a C_0 = concentration at 0 min. $T_{1/2}$ = half-life. AUC = area under the plasma concentration time curve. V_{ss} = volume of distribution at steady state. Cl_p = clearance; MRT = mean residence time.



* Control

Figure 6. Compound **26** in vivo biomarker profile at 25 mg/kg, iv, single dose. Tumor tissue from the MDA-361 xenograft model was examined for p-Akt suppression and induction of cleaved PARP at different time points. The p70 pS6K and pS6 panels show suppression of phosphorylation of these mTOR effector proteins.

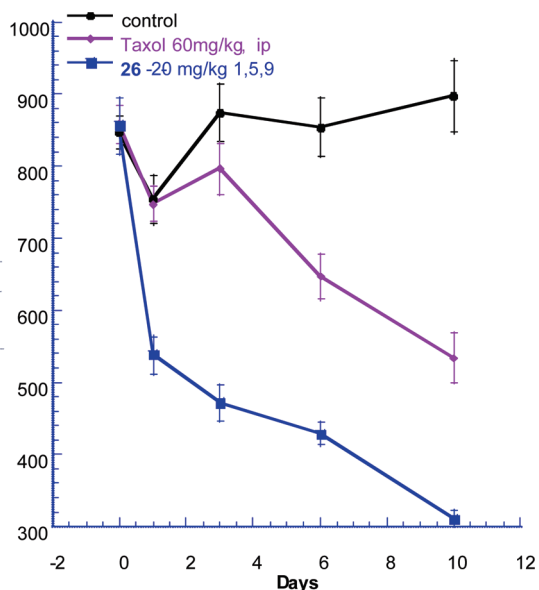


Figure 7. Efficacy profile of compound **26** in MDA-361 xenograft model. Shown is the tumor regression caused by **26** at 20 mg/kg, iv, on days 1, 5, 9 and by paclitaxel (Taxol) at 60 mg/kg, ip (single dose). Y axis represents tumor volume in mm³.

We have also discovered that the presence of an amide functionality bearing water solubilizing groups boosted potency, both in enzyme and in cell proliferation assays. During our course of optimization, we identified compound **26**, which has shown excellent efficacy especially in in vivo xenograft models. Compound **26** is currently entering phase I clinical trials as a single agent for iv administration.

Experimental Section

General Methods. Melting points were determined in open capillary tubes on a Mel-Temp melting point apparatus and are uncorrected. ¹H NMR spectra were determined with a Bruker DPX-400 spectrometer at 400 MHz. Chemical shifts are

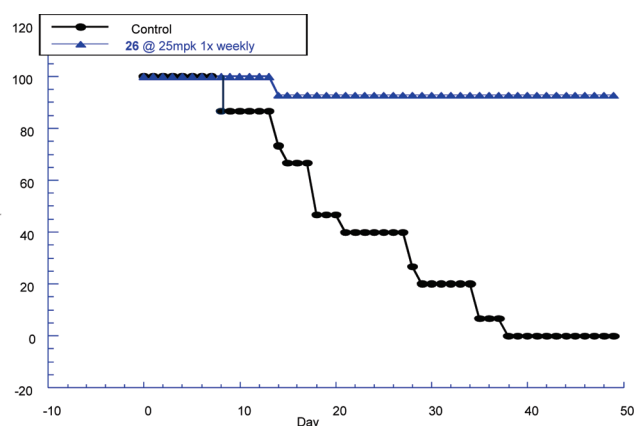


Figure 8. Orthotopic model for compound **26** in H1975 (non-small-cell lung carcinoma). Compound **26** was given once weekly for 7 weeks at 25 mg/kg. The Y axis represents % survival (Kaplan–Meier plot).²⁷

reported in parts per million (δ) relative to residual chloroform (7.26 ppm), TMS (0 ppm), or dimethyl sulfoxide (2.49 ppm) as an internal reference with coupling constants (J) reported in hertz (Hz). The peak shapes are denoted as follows: s, singlet; d, doublet; t, triplet; q, quartet; m, multiplet; br, broad. Electrospray (ES) mass spectra were recorded in positive or negative mode on a Micromass Platform spectrometer. Electron impact (EI) and high-resolution mass spectra were obtained on a Finnigan MAT-90 spectrometer. Combustion analyses were obtained using Perkin-Elmer series II 2400 CHNS/O analyzer. The purity of compounds **8–32** was determined by analytical LC/MS using an Agilent 1100 LC equipped with an Agilent MSD mass spectrometer and by analytical LC using an X-Bridge BEH column, MeOH/H₂O eluent at 1 mL/min flow (containing 0.05% NH₄OAc), 20 min gradient from 10% MeOH to 90% ACN, monitored by UV absorption at 215 nm. The purity of all the above-mentioned compounds was found to be >95%. Reverse phase HPLC purifications were performed on a Gilson preparative HPLC system controlled by Unipoint software, using a Phenomenex Gemini 100 mm × 30.0 mm column. Thin-layer chromatography (TLC) was performed on Merck PLC prescored plates ₆₀F₂₅₄. The terms “concentrated” and “evaporated” refer to removal of solvents using a rotary evaporator at water aspirator pressure with a bath temperature equal to or less than 40 °C. Unless otherwise noted, reagents were obtained from commercial sources and were used without further purification.

Modeling. The homology model was built with Prime 1.6 with 3IBE^{21a} as the template. Docking studies were performed using Glide, version 4.5 initially and version 5.5 more recently. Docking studies were performed either without constraints or with a hydrogen bonding constraint to the backbone-NH of Val851. Figures 2, 3, and 4 were made using PyMOL: Prime, version 1.6 (2007) (Schrodinger, LLC, New York, NY); Glide, version 5.5 (2009) (Schrodinger, LLC, New York, NY); and PyMOL Molecular Graphics System (2008) (W. L. DeLano; DeLano Scientific LLC, Palo Alto, CA).

Preparation of 1-[4-(4,6-Dimorpholin-4-yl-1,3,5-triazin-2-yl)phenyl]-3-phenylurea (8). Step 1: Preparation of 2-Chloro-4,6-dimorpholin-4-yl[1,3,5]triazine (6). To a stirred solution of cyanuric chloride (18.4 g, 10 mmol) in acetone (100 mL) and

crushed ice (500 g), a mixture of triethylamine (30.0 g, excess) and morpholine (17.4 g, 20 mmol) was added at $-10\text{ }^{\circ}\text{C}$. After the addition, the reaction mixture was stirred at room temperature for 1 h and diluted with 50 mL of water. Separated white solid was filtered and washed with water. The white solid was dried and filtered. The crude product was found to be pure and taken to the next step without purification (25 g, 87% yield). (M + H) 286.7

Step 2: Preparation of 4-(4,6-Dimorpholin-4-yl-1,3,5-triazin-2-yl)aniline (7). A mixture of 2-chloro-4,6-dimorpholin-4-yl-[1,3,5]triazine (1.4 g, 4.9 mmol), a catalytic amount of tetrakis-(triphenylphosphine)palladium(0) (70 mg, 0.061 mmol), sodium carbonate solution 2 M (3 mL), 4-aminophenylboronic acid pinacol ester (1.6 g, 7.3 mmol), and DME (100 mL) was refluxed for 24 h. The solvent was evaporated, and the residue was dissolved in methylene chloride and filtered through Celite. The filtrate was washed with water (200 mL), and the organic layer was dried with magnesium sulfate. This was filtered, and the solvent was evaporated. The residue was purified by SiO_2 column chromatography and eluted with ethyl acetate/hexanes (1:1) to give of 4-(4,6-dimorpholin-4-yl-1,3,5-triazin-2-yl)aniline (1.40 g, 83% yield) as an amorphous solid. (M + H) 343.

Step 3: Preparation of 1-[4-(4,6-Dimorpholin-4-yl-1,3,5-triazin-2-yl)phenyl]-3-phenylurea (8). To a stirred mixture of 4-(4,6-dimorpholin-4-yl-1,3,5-triazin-2-yl)aniline (140 mg, 0.40 mmol) and a catalytic amount of dimethylaminopyridine (DMAP) in methylene chloride (100 mL) was added a small excess of phenyl isocyanate (59.5 mg, 0.50 mmol). The mixture was stirred at room temperature for 48 h. The reaction mixture was concentrated to half of its original volume, and the separated precipitate was collected by filtration and washed with methanol (15 mL) and then with diethyl ether. In some cases the crude product obtained was purified by SiO_2 column chromatography by eluting it with 10% ethyl acetate/hexane (128 mg, 68% yield). White solid. 462.3 (M + H). Purity by analytical HPLC 99.3%. (Prodigy ODS3, 0.46 cm \times 15 cm, 20 min gradient acetonitrile in water, trifluoroacetic acid, detector wavelengths, 215 and 254 nm.) ^1H NMR (DMSO- d_6) δ 3.6 (m, 8H), 3.7 (m, 8H), 7.0 (t, $J = 7.0$ Hz, 1H), 7.3 (t, $J = 7.3$ Hz, 2H), 7.5 (d, $J = 8.1$ Hz, 2H), 7.6 (d, $J = 8.8$ Hz, 2H), 8.3 (d, $J = 8.6$ Hz, 2H), 8.7 (s, 1H), 9.0 (s, 1H) ppm.

Preparation of 1-[4-(4,6-Dimorpholin-4-yl-1,3,5-triazin-2-yl)phenyl]-3-ethylurea (9). Starting from 4-(4,6-dimorpholin-4-yl-1,3,5-triazin-2-yl)aniline (0.130 g 0.38 mmol) and ethyl isocyanate (260 mg, 10-fold excess) and following the procedure outlined for compound 8, the title compound was isolated as a white solid (38 mg, 25% yield). (M + H) 414.3. Purity by analytical HPLC 97.8%. (Prodigy ODS3, 0.46 cm \times 15 cm, 20 min gradient acetonitrile in water, trifluoroacetic acid, detector wavelengths, 215 and 254 nm.) ^1H NMR (DMSO- d_6) δ 3.6 (m, 8H), 3.7 (m, 8H), 3.75 (t, $J = 6.8$ Hz, 3H), 3.8 (q, $J = 6.8$ Hz, 2H), 7.6 (d, 2H, $J = 8.3$ Hz), 8.2 (d, 2H, $J = 8.3$ Hz), 8.9 (broad s, 2H) ppm.

Preparation of 1-[4-(4,6-Dimorpholin-4-yl-1,3,5-triazin-2-yl)phenyl]-3-(4-fluorophenyl)urea (11). Starting from 4-(4,6-dimorpholin-4-yl-1,3,5-triazin-2-yl)aniline (0.140 g 0.40 mmol) and 4-fluorophenyl isocyanate (83 mg, 0.61 mmol) and following the procedure outlined in example 8, 65 mg (33% yield) of the title product was isolated as white solid. (M + H) 480.3. Purity by analytical HPLC 97.9%. (Prodigy ODS3, 0.46 cm \times 15 cm, 20 min gradient acetonitrile in water, trifluoroacetic acid, detector wavelengths, 215 and 254 nm.) ^1H NMR (DMSO- d_6) δ 3.6 (m, 8H), 3.7 (m, 8H), 7.2 (t, $J = 8.3$ Hz, 2H), 7.4 (m, 2H), 7.5 (d, $J = 9.3$ Hz, 2H), 8.3 (d, $J = 9.1$ Hz, 2H), 8.8 (s, 1H), 9.0 (s, 1H) ppm.

Preparation of 1-[4-(4,6-Dimorpholin-4-yl-1,3,5-triazin-2-yl)phenyl]-3-(4-methylphenyl)urea (12). Starting from 4-(4,6-dimorpholin-4-yl-1,3,5-triazin-2-yl)aniline (0.140 g 0.40 mmol) and 4-methylphenyl isocyanate (74 mg, 0.56 mmol) and following the procedure outlined for the preparation of compound 8,

the title compound was isolated as a white solid (65 mg, 33% yield). (M + H) 476.4. Purity by analytical HPLC 98.2%. (Prodigy ODS3, 0.46 cm \times 15 cm, 20 min gradient acetonitrile in water, trifluoroacetic acid, detector wavelengths, 215 and 254 nm.) ^1H NMR (DMSO- d_6) δ 3.6 (m, 8H), 3.7 (m, 8H), 2.5 (s, 3H), 7.1 (d, $J = 9.6$ Hz, 2H), 7.3 (d, $J = 8.3$ Hz, 2H), 7.6 (d, $J = 8.6$ Hz, 2H), 8.2 (d, $J = 9.6$ Hz, 2H), 8.6 (s, 1H), 8.9 (s, 1H) ppm.

Preparation of 1-(4-Chlorophenyl)-3-[4-(4,6-dimorpholin-4-yl-1,3,5-triazin-2-yl)phenyl]urea (13). Starting from 4-(4,6-dimorpholin-4-yl-1,3,5-triazin-2-yl)aniline (0.140 g 0.40 mmol) and 4-chlorophenyl isocyanate (94 mg, 0.61 mmol) and following the procedure outlined for the preparation of 8, the title compound was isolated as a white solid (60 mg, 30% yield). (M + H) 496.3. Purity by analytical HPLC 96.8%. (Prodigy ODS3, 0.46 cm \times 15 cm, 20 min gradient acetonitrile in water, trifluoroacetic acid, detector wavelengths, 215 and 254 nm.) ^1H NMR (DMSO- d_6) δ 3.6 (m, 8H), 3.7 (m, 8H), 7.1 (m, 2H), 7.4 (m, $J = 8.1$ Hz, 2H), 7.6 (d, $J = 8.8$ Hz, 2H), 8.2 (d, $J = 8.3$ Hz, 2H), 8.8 (s, 1H), 9.0 (s, 1H) ppm.

Preparation of (2,4-Difluorophenyl)-3-[4-(4,6-dimorpholin-4-yl-1,3,5-triazin-2-yl)phenyl]urea (14). Starting from 4-(4,6-dimorpholin-4-yl-1,3,5-triazin-2-yl)aniline (0.105 g 0.30 mmol) and 2,4-difluorophenyl isocyanate (71 mg, 0.45 mmol) and following the procedure outlined in example 8, the title compound was isolated as a white solid (40 mg, 27% yield). (M + H) 498.4. Purity by analytical HPLC 97.5%. (Prodigy ODS3, 0.46 cm \times 15 cm, 20 min gradient acetonitrile in water, trifluoroacetic acid, detector wavelengths, 215 and 254 nm.) ^1H NMR (DMSO- d_6) δ 3.65 (m, 8H), 3.8 (b, 8H), 7.04 (m, 1H), 7.32 (m, 1H), 7.54 (d, $J = 8.6$ Hz, 2H), 8.07 (m, 1H), 8.1 (d, $J = 8.2$ Hz, 2H), 8.57 (s, 1H), 9.32 (s, 1H) ppm.

Preparation of 1-[4-(4,6-Dimorpholin-4-yl-1,3,5-triazin-2-yl)phenyl]-3-[4-(1-hydroxyethyl)phenyl]urea (16). To a stirred mixture of 4-(4,6-dimorpholin-4-yl-1,3,5-triazin-2-yl)aniline (0.140, 0.40 mmol) in methylene chloride at $0\text{ }^{\circ}\text{C}$ was added triphosgene (0.25, 0.84 mmol) and Et_3N (3 mL). The reaction mixture was stirred for 20 min at $0\text{ }^{\circ}\text{C}$. Then 1-(4-aminophenyl)ethanol (0.10 g, 0.73 mmol) was added to the mixture. The reaction mixture was stirred for about 16 h at room temperature. The solvent was removed. The residue was dissolved in DMSO and placed in an HPLC instrument, with acetonitrile buffer TFA to give [4-(4,6-dimorpholin-4-yl-1,3,5-triazin-2-yl)phenyl]-3-[4-(1-hydroxyethyl)phenyl]urea (48 mg, 24% yield). (M + H) 506.4. Purity by analytical HPLC 95.5%. (Prodigy ODS3, 0.46 cm \times 15 cm, 20 min gradient acetonitrile in water, trifluoroacetic acid, detector wavelengths, 215 and 254 nm.) ^1H NMR (DMSO- d_6) δ 2.66 (t, $J = 7.1$ Hz, 2H), 3.43 (b, 1H), 3.57 (t, $J = 7.6$, 2H), 3.66 (m, 8H), 3.81 (b, 8H), 7.13 (d, $J = 8.1$ Hz, 2H), 7.36 (d, $J = 8.3$ Hz, 2H), 7.54 (d, $J = 8.8$ Hz, 2H), 8.27 (d, $J = 8.26$ Hz, 2H), 8.63 (s, 1H), 8.95 (s, 1H) ppm.

Preparation of 1-[4-(4,6-Dimorpholin-4-yl-1,3,5-triazin-2-yl)phenyl]-3-[4-(hydroxymethyl)phenyl]urea (15). Starting from 4-(4,6-dimorpholin-4-yl-1,3,5-triazin-2-yl)aniline (0.140, 0.40 mmol) and 4-aminophenylmethanol (100 mg, 0.81 mmol) and following the procedure described in example 16, 1-[4-(4,6-dimorpholin-4-yl-1,3,5-triazin-2-yl)phenyl]-3-[4-(hydroxymethyl)phenyl]urea was isolated by HPLC purification (58 mg, 26% yield). (M + H) (ESI) $m/z = 492.3$. Purity by analytical HPLC 95.8%. (Prodigy ODS3, 0.46 cm \times 15 cm, 20 min gradient acetonitrile in water, trifluoroacetic acid, detector wavelengths, 215 and 254 nm.) ^1H NMR (DMSO- d_6) δ 3.43 (b, 1H), 3.66 (m, 8H), 3.81 (b, 8H), 4.43 (s, 2H), 7.23 (d, $J = 8.8$ Hz, 2H), 7.41 (d, $J = 8.3$ Hz, 2H), 7.55 (d, $J = 8.6$ Hz, 2H), 8.27 (d, $J = 8.8$ Hz, 2H), 8.7 (s, 1H), 8.98 (s, 1H) ppm.

Preparation of 1-[4-(4,6-Dimorpholin-4-yl-1,3,5-triazin-2-yl)phenyl]-3-thiophen-2-ylurea (17). Starting from 4-(4,6-dimorpholin-4-yl-1,3,5-triazin-2-yl)aniline (60 mg, 0.17 mmol) and 2-thienyl isocyanate (18 mg, 0.14 mmol) and following the procedure as outlined in example 8, the title compound was isolated as a gray solid after SiO_2 column chromatography by

eluting with 5% ethyl acetate/methanol. (12 mg, 14% yield). (M + H) = 468.3. Purity by analytical HPLC 96.9%. (Prodigy ODS3, 0.46 cm × 15 cm, 20 min gradient acetonitrile in water, trifluoroacetic acid, detector wavelengths, 215 and 254 nm.) ¹H NMR (DMSO-*d*₆) δ 3.66 (m, 8H), 3.81 (b, 8H), 6.58 (dd, *J* = 1.3 Hz, *J* = 3.8 Hz, 1H), 6.82 (dd, *J* = 3.8 Hz, *J* = 5.8 Hz, 1H), 6.9 (dd, *J* = 1.3 Hz, *J* = 5.8 Hz, 1H), 7.55 (d, *J* = 8.6 Hz, 2H), 8.28 (d, *J* = 8.6 Hz, 2H), 9.05 (s, 1H), 9.68 (s, 1H), ppm.

Preparation of 1-[4-(4,6-Dimorpholin-4-yl-1,3,5-triazin-2-yl)phenyl]-3-pyridin-3-ylurea (18). Starting from 4-(4,6-dimorpholin-4-yl-1,3,5-triazin-2-yl)aniline (0.08 g 0.23 mmol) and 3-pyridyl isocyanate (30 mg, 0.25 mmol) and following the procedure as outlined in example 8, the title compound was isolated as a white solid. The product was purified by SiO₂ column chromatography by eluting it with 10% methanol/ethyl acetate. (60 mg, 56% yield). (M + H) 463.2. Purity by analytical HPLC 98.2%. (Prodigy ODS3, 0.46 cm × 15 cm, 20 min gradient acetonitrile in water, trifluoroacetic acid, detector wavelengths, 215 and 254 nm.) ¹H NMR (DMSO-*d*₆) δ 3.66 (m, 8H), 3.82 (b, 8H), 7.33 (m, 1H), 7.56 (d, *J* = 8.6 Hz, 2H), 7.96 (d, *J* = 8.8 Hz, 1H), 8.21 (d, *J* = 5.3 Hz, 1H), 8.58 (d, *J* = 8.3 Hz, 2H), 8.61 (d, *J* = 2.5 Hz, 1H), 8.91 (s, 1H), 9.13 (s, 1H), ppm.

Preparation of 1-[4-(4,6-Dimorpholin-4-yl-1,3,5-triazin-2-yl)phenyl]-4-pyridin-4-ylurea (19). To a mixture of 4-(4,6-dimorpholin-4-yl-1,3,5-triazin-2-yl)aniline (0.20 g 0.40 mmol) in methylene chloride (80 mL) at 0 °C was added triphosgene (0.25 mg, 0.84 mmol) and triethylamine (3 mL). The mixture was stirred for 20 min at 0 °C, and 4-aminopyridine (0.10 g 0.83 mmol) was added to the reaction mixture. The mixture was stirred for another 2 h at room temperature. The solvent was evaporated and the residue was submitted to HPLC using acetonitrile/TFA as mobile phase to give 1-[4-(4,6-dimorpholin-4-yl-1,3,5-triazin-2-yl)phenyl]-3-pyridin-4-ylurea (98.2 mg 36% yield). (M + H) 463.4. Purity by analytical HPLC 97.9%. (Prodigy ODS3, 0.46 cm × 15 cm, 20 min gradient acetonitrile in water, trifluoroacetic acid, detector wavelengths, 215 and 254 nm.) ¹H NMR (DMSO-*d*₆) δ 3.51 (b, 8H), 3.64 (b, 8H), 7.60 (d, *J* = 8.6 Hz, 2H), 7.92 (d, *J* = 7.3 Hz, 2H), 8.32 (d, *J* = 8.8 Hz, 2H), 8.58 (d, *J* = 7.6 Hz, 2H), 9.79 (s, 1H), 10.54 (s, 1H) ppm.

Preparation of 1-[4-(4,6-Dimorpholin-4-yl-1,3,5-triazin-2-yl)phenyl]-3-pyridazin-4-ylurea (20). To a mixture of 4-(4,6-dimorpholin-4-yl-1,3,5-triazin-2-yl)aniline (50 mg 0.15 mmol) in methylene chloride (80 mL) at 0 °C was added triphosgene (26 mg, 0.088 mmol) and triethylamine (0.2 mL). The mixture was stirred for 20 min at 0 °C. Pyridazine-4-amine (42 mg 0.48 mmol) was added to the reaction mixture, and the mixture was stirred for another 2 h at room temperature. The solvent was evaporated and the residue was submitted to the HPLC using acetonitrile/NH₃ as mobile phase to give 17 mg (25% yield) of 1-[4-(4,6-dimorpholin-4-yl-1,3,5-triazin-2-yl)phenyl]-3-pyridazin-4-ylurea. (M + H) 464.2. Purity by analytical HPLC 95.6%. (Prodigy ODS3, 0.46 cm × 15 cm, 20 min gradient acetonitrile in water, trifluoroacetic acid, detector wavelengths, 215 and 254 nm.) ¹H NMR (DMSO-*d*₆) δ 3.6 (m, 8H), 3.7 (m, 8H), 7.5 (d, *J* = 9.4 Hz, 1H), 7.81–7.84 (m, 2H), 8.3 (d, *J* = 8.3 Hz, 2H), 8.9 (d, *J* = 6.4 Hz, 2H), 9.1 (m, 1H), 9.4 (s, 1H) ppm.

Preparation of Methyl 4-(3-(4-(4,6-Dimorpholino-1,3,5-triazin-2-yl)phenyl)ureido)benzoate (21). Starting from 4-(4,6-dimorpholin-4-yl-1,3,5-triazin-2-yl)aniline (342 mg, 1.0 mmol) and methyl 4-isocyanatobenzoate (177 mg, 1 mmol) and following the procedure as outlined in example 8, the title compound was isolated as a gray solid (480 mg, 92%) after SiO₂ column chromatography by eluting with 50% ethyl acetate/hexane. (M + H) 520.3. Purity by analytical HPLC 95.3%. (Prodigy ODS3, 0.46 cm × 15 cm, 20 min gradient acetonitrile in water, trifluoroacetic acid, detector wavelengths, 215 and 254 nm.) ¹H NMR (DMSO-*d*₆) δ 3.6 (m, 8H), 3.7 (m, 8H), 3.8 (s, 3H), 7.57–7.62 (m, 2H), 7.8 (d, *J* = 7.6 Hz, 4H), 8.3 (d, *J* = 9.1 Hz, 2H), 9.11–9.15 (d, *J* = 12.6 Hz, 2H) ppm.

Preparation of 4-[3-(4-(4,6-Dimorpholino-1,3,5-triazin-2-yl)phenyl)ureido]benzoic Acid (22). To a stirred mixture of methyl 4-(3-(4-(4,6-dimorpholino-1,3,5-triazin-2-yl)phenyl)ureido)benzoate (1.4 g, 2.69 mmol), THF (10 mL), MeOH (5 mL), and H₂O (2.5 mL) was added LiOH · H₂O (339 mg, 8.07 mmol). The mixture was then heated under reflux for 8 h and concentrated. H₂O (5 mL) was added, and the mixture was then acidified with 2 N HCl. The solid was filtered, washed with H₂O, and dried to give the product as a tan solid, which was taken to next step without purification (1.3 g, 96% yield). MS (ESI) *m/z* = 506.2. Purity by analytical HPLC 98.4%. (Prodigy ODS3, 0.46 cm × 15 cm, 20 min gradient acetonitrile in water, trifluoroacetic acid, detector wavelengths, 215 and 254 nm.) ¹H NMR (DMSO-*d*₆) δ 3.6 (m, 8H), 3.7 (m, 8H), 7.56–7.59 (m, 4H), 7.9 (d, *J* = 8.6 Hz, 2H), 8.3 (d, *J* = 7.6 Hz, 2H), 9.31–9.34 (d, *J* = 10.8 Hz, 2H) ppm.

Preparation of *N*-[2-(Dimethylamino)ethyl]-4-([4-(4,6-dimorpholin-4-yl-1,3,5-triazin-2-yl)phenyl]carbonyl)aminobenzamide (24). A solution of 4-[3-(4-(4,6-dimorpholino-1,3,5-triazin-2-yl)phenyl)ureido]benzoic acid (150 mg, 0.297 mmol), Hunig's base (303 μL, 1.782 mmol), and HBTU (563 mg, 1.485 mmol) in 2 mL of NMP was stirred for 1 h at room temperature. *N,N'*-Dimethylethane-1,2-diamine (130 μL, 1.188 mmol) was added, and then the mixture was stirred overnight. At the end, CH₂Cl₂ (40 mL) was added and washing was done with saturated NaHCO₃ and H₂O. The mixture was concentrated and purified by silica gel chromatography, with CH₂Cl₂/methanol/7N NH₃ in MeOH (10:1:0.22) to give the product as a white solid (98 mg, 57% yield). MS (ESI) *m/z* = 576.4, MS (ESI) *m/z* 288.7. HRMS: calcd for C₂₉H₃₇N₉O₄ + H⁺, 576.3041; found 576.3036. Purity by analytical HPLC 98.4%. (Prodigy ODS3, 0.46 cm × 15 cm, 20 min gradient acetonitrile in water, trifluoroacetic acid, detector wavelengths, 215 and 254 nm.) ¹H NMR (DMSO-*d*₆) δ 3.6 (m, 8H), 3.7 (m, 8H), 2.5 (s, 6H), 2.8 (d, *J* = 5.3 Hz, 2H), 3.2 (q, *J* = 5.3 Hz, 2H), 7.55–7.58 (m, 4H), 7.8 (d, *J* = 9.1 Hz, 2H), 8.2 (d, *J* = 8.8 Hz, 2H), 8.6 (m, 1H), 9.6 (s, 1H), 9.7 (broad s, 1H) ppm.

Preparation of 4-(3-(4-(4,6-Dimorpholino-1,3,5-triazin-2-yl)phenyl)ureido)-*N*-methylbenzamide (23). A solution of 4-(3-(4-(4,6-dimorpholino-1,3,5-triazin-2-yl)phenyl)ureido)benzoic acid (150 mg, 0.297 mmol), Hunig's base (303 μL, 1.782 mmol), and HBTU (563 mg, 1.485 mmol) in 2 mL of NMP was reacted according to example 24 with methylamine (594 μL, 2 M solution in THF) to give the product as a white solid (118 mg, 77% yield). MS (ESI) *m/z* = 519.3. HRMS: calcd for C₂₆H₃₀N₈O₄ + H⁺, 519.2463; found 519.2456. Purity by analytical HPLC 95.7%. (Prodigy ODS3, 0.46 cm × 15 cm, 20 min gradient acetonitrile in water, trifluoroacetic acid, detector wavelengths, 215 and 254 nm.) ¹H NMR (DMSO-*d*₆) δ 3.6 (m, 8H), 3.7 (m, 8H), 2.81 (d, *J* = 3.8 Hz, 3H), 7.51–7.57 (m, 4H), 7.8 (d, *J* = 7.3 Hz, 2H), 8.3 (d, *J* = 7.6 Hz, 2H), 8.9 (s, 1H), 9.9 (s, 1H) ppm.

Preparation of 1-[4-(4,6-Dimorpholino-1,3,5-triazin-2-yl)phenyl]-3-{4-[(4-methylpiperazine-1-yl)carbonyl]phenyl}urea Hydrochloride (25). A stirred solution of 4-(3-(4-(4,6-dimorpholino-1,3,5-triazin-2-yl)phenyl)ureido)benzoic acid (150 mg, 0.297 mmol), Hunig's base (303 μL, 1.782 mmol), and HBTU (563 mg, 1.485 mmol) in 2 mL of NMP was reacted according to example 24 with 1-methylpiperazine (132 μL, 1.188 mmol) to give 1-(4-(4,6-dimorpholino-1,3,5-triazin-2-yl)phenyl)-3-(4-(4-methylpiperazine-1-carbonyl)phenyl)urea as a white solid (95 mg, 54% yield). MS (ESI) *m/z* = 588.4 and 294.7. HRMS: calcd for C₃₀H₃₇N₉O₄ + H⁺, 588.3041; found (ESI, [M + H]⁺ obsd), 588.3033. Purity by analytical HPLC 98.2%. (Prodigy ODS3, 0.46 cm × 15 cm, 20 min gradient acetonitrile in water, trifluoroacetic acid, detector wavelengths, 215 and 254 nm.) ¹H NMR (DMSO-*d*₆) δ 2.2 (s, 3H), 2.5 (m, 4H), 3.3 (m, 4H), 3.6 (m, 8H), 3.7 (m, 8H), 7.3 (d, *J* = 8.3 Hz, 2H), 7.51–7.58 (m, 4H), 8.3 (d, *J* = 9.0 Hz, 2H), 8.9 (s, 1H), 9.1 (s, 1H) ppm. To 1-(4-(4,6-dimorpholino-1,3,5-triazin-2-yl)phenyl)-3-(4-(4-methylpiperazine-1-carbonyl)phenyl)urea

(70 mg, 0.119 mmol) and MeOH (1 mL) was added 4 N HCl in dioxane (1 mL), and the mixture was stirred for 3 h. The solid was filtered and washed with ether to give the product as a white solid (74 mg, 100% yield).

Preparation of 1-(4-{[4-(Dimethylamino)piperidin-1-yl]carbonyl}phenyl)-3-[4-(4,6-dimorpholino-4-yl-1,3,5-triazin-2-yl)phenyl]urea (26). A solution of 4-(3-(4-(4,6-dimorpholino-1,3,5-triazin-2-yl)phenyl)ureido)benzoic acid (50 mg, 0.099 mmol), Hunig's base (103 μ L, 0.594 mmol), and HBTU (188 mg, 0.495 mmol) in 2 mL of NMP was reacted according to example 24 with *N,N*-dimethylpiperidin-4-amine (51 mg, 0.396 mmol). The solvent was evaporated and purified by HPLC to give the product (30.6 mg, 52% yield). MS (ESI) m/z = 616.7. HRMS: calcd for $C_{32}H_{41}N_9O_4 + H^+$, 616.33543; found (ESI-FTMS, $[M + H]^+$), 616.33424. Purity by analytical HPLC 99.3%. (Prodigy ODS3, 0.46 cm \times 15 cm, 20 min gradient acetonitrile in water, trifluoroacetic acid, detector wavelengths, 215 and 254 nm.) 1H NMR (DMSO- d_6) δ 1.29–1.36 (m, 6H), 2.6 (m, 4H), 2.9 (m, 1H), 3.3 (m, 4H), 3.6 (m, 8H), 3.7 (m, 8H), 7.3 (d, J = 8.3 Hz, 2H), 7.51–7.57 (m, 4H), 8.3 (d, J = 8.3 Hz 2H), 8.9 (s, 1H), 9.0 (s, 1H) ppm. Anal. Calcd for $C_{32}H_{41}N_9O_4$: C 62.42%, H 6.71%, N 20.47%. Found: C 62.34%, H 6.67%, N 20.39%.

Preparation of 1-[4-(4,6-Dimorpholino-4-yl-1,3,5-triazin-2-yl)-phenyl]-3-{4-[(4-pyrrolidin-1-yl)piperidin-1-yl]carbonyl}phenyl]urea (27). Compound 27 was prepared by reacting 4-(3-(4-(4,6-dimorpholino-1,3,5-triazin-2-yl)phenyl)ureido)benzoic acid and 4-pyrrolidin-1-ylpiperidine. (M + H) m/z = 642.3. HRMS: calcd for $C_{34}H_{43}N_9O_4 + H^+$, 642.3510; found (ESI-FTMS, $[M + H]^+$), 642.3491. Purity by analytical HPLC 97.2%. (Prodigy ODS3, 0.46 cm \times 15 cm, 20 min gradient acetonitrile in water, trifluoroacetic acid, detector wavelengths, 215 and 254 nm.) 1H NMR (DMSO) δ 1.62 (m, 2H), 1.86 (m, 2H), 1.98 (m, 2H), 2.08 (m, 2H), 2.94 (brs, 2H), 3.07 (m, 2H), 3.38 (m, 1H), 3.48 (m, 2H), 3.72–4.01 (m, 17H), 7.35 (d, J = 8.8 Hz, 2H), 7.55 (d, J = 8.8 Hz, 2H), 7.57 (d, J = 8.8 Hz, 2H), 8.28 (d, J = 8.8 Hz, 2H), 9.33 (s, 1H), 9.37 (s, 1H), 10.43 (m, 1H) ppm.

Preparation of 1-(4-(1,4'-Bipiperidine-1'-carbonyl)phenyl)-3-(4-(4,6-dimorpholino-1,3,5-triazin-2-yl)phenyl)urea (28). A solution of 4-(3-(4-(4,6-dimorpholino-1,3,5-triazin-2-yl)phenyl)ureido)benzoic acid (50 mg, 0.099 mmol), Hunig's base (103 μ L, 0.594 mmol), and HBTU (188 mg, 0.495 mmol) in 2 mL of NMP was reacted according to example 24 with 1,4'-bipiperidine (67 mg, 0.396 mmol). The solvent was evaporated and purified by HPLC to give the product as a white solid (39 mg, 60% yield). MS (ESI) m/z = 656.8.

Preparation of *N*-(2-(Dimethylamino)ethyl)-4-(3-(4-(4,6-dimorpholino-1,3,5-triazin-2-yl)phenyl)ureido)-*N*-methylbenzamide Hydrochloride (30). A stirred solution of 4-(3-(4-(4,6-dimorpholino-1,3,5-triazin-2-yl)phenyl)ureido)benzoic acid (150 mg, 0.297 mmol), Hunig's base (303 μ L, 1.782 mmol), and HBTU (563 mg, 1.485 mmol) in 2 mL of NMP was reacted according to example 24 with N^1,N^1,N^2 -trimethylethane-1,2-diamine (154 μ L, 1.188 mmol) to give *N*-(2-(dimethylamino)ethyl)-4-(3-(4-(4,6-dimorpholino-1,3,5-triazin-2-yl)phenyl)ureido)-*N*-methylbenzamide as a white solid (88 mg, 50% yield). MS (ESI) m/z = 590.2.

To *N*-(2-(dimethylamino)ethyl)-4-(3-(4-(4,6-dimorpholino-1,3,5-triazin-2-yl)phenyl)ureido)-*N*-methylbenzamide (55 mg, 0.127 mmol) and MeOH (1 mL) was added 4 N HCl in dioxane (1 mL), and the mixture was stirred for 3 h. The solid was filtered and washed with ether to give the product as a white solid (70 mg, yield = 88%). HRMS: calcd for $C_{30}H_{39}N_9O_4 + H^+$, 590.3198; found (ESI-FTMS, $[M + H]^+$), 590.3194. Purity by analytical HPLC 99.8%. (Prodigy ODS3, 0.46 cm \times 15 cm, 20 min gradient acetonitrile in water, trifluoroacetic acid, detector wavelengths, 215 and 254 nm.)

Acknowledgment. The authors thank members of the Wyeth Chemical Technologies Group for analytical and spectral determinations, Dr. Joseph Marini and Angela Bretz

for nude mouse microsome assays, and Dr. Li Di and Susan Li for human microsome assays.

References

- (1) (a) Vivanco, I.; Sawyers, C. L. The phosphatidylinositol-3-kinase Akt pathway in human cancer. *Nat. Rev. Cancer* **2002**, *2*, 489–501. (b) Liu, P.; Cheng, H.; Roberts, T. M.; Zhao, J. J. Targeting the phosphoinositide 3-kinase pathway in cancer. *Nat. Rev.* **2009**, *8*, 627–644. (c) Lempiainen, H.; Halazonetis, T. D. Emerging common themes in regulation of PIKKS and PI3Ks. *EMBO J.* **2009**, *28*, 3067–3073.
- (2) Yap, T. A.; Garrett, M. D.; Walton, M. I.; Raynand, F.; deBono, J. S.; Workman, P. Targeting the PI3K-Akt-mTOR pathway, progress, pitfalls and promises. *Curr. Opin. Pharmacol.* **2008**, *8*, 393–414.
- (3) Bellacosa, A.; Kumar, C. C.; Dieristofano, A.; Testa, J. R. Activation of Akt kinases in cancer: implications for therapeutic targeting. *Adv. Cancer Res.* **2005**, *94*, 29–86.
- (4) Manning, B. D.; Cantley, L. C. Akt/PKB signaling: navigating down stream. *Cell* **2007**, *129*, 1261–1274.
- (5) Engelman, J. A.; Luo, J.; Cantley, L. C. The evolution of phosphatidylinositol 3-kinases as regulators of growth and metabolism. *Nat. Rev. Genet.* **2006**, *7*, 606–619.
- (6) Hennessy, B. T.; Smith, D. L.; Ram, P. T.; Lu, Y.; Mills, G. B. Exploiting the PI3K/Akt pathway for cancer drug discovery. *Nat. Rev. Drug Discovery* **2005**, *4*, 988–1004.
- (7) Maehama, T.; Dixon, J. E. The tumor suppressor, PTEN/MMAC1, dephosphorylates the lipid second messenger, phosphatidylinositol 3,4,5-triphosphate. *J. Biol. Chem.* **1998**, *273*, 13375–13378.
- (8) Ali, I. U.; Schriml, L. M.; Dean, M. Mutational spectra of PTEN/MMAC1 gene: a tumor suppressor with lipid phosphatase activity. *J. Natl. Cancer Inst.* **1999**, *91*, 1922–1932.
- (9) Shayesteh, L.; Kuo, W.; Baldocchi, R.; Godfrey, T.; Collins, C.; Pinkel, D.; Powell, B.; Mills, G. B.; Gray, J. W. PIK3CA is implicated as an oncogene in ovarian cancer. *Nat. Genet.* **1999**, *21*, 99–102.
- (10) Samuels, Y.; Wang, Z.; Bardelli, A.; Silliman, N.; Ptak, J.; Szabo, S.; Yan, H.; Gazdar, A.; Powell, S. M.; Riggins, G. J.; Wilson, J. K.; Markowitz, S.; Kinzler, K. W.; Vogelstein, B.; Velculescu, V. E. High frequency mutations of the PIK3CA gene in human cancers. *Science* **2004**, *30*, 554.
- (11) Parsons, D. W.; Wang, T. L.; Samuels, Y.; Bardelli, A.; Cummins, J. M.; De Long, L.; Silliman, N.; Ptak, J.; Szabo, S.; Wilson, J. K.; Markowitz, S.; Kinzler, K. W.; Vogelstein, B.; Lengauer, C.; Velculescu, V. E. Colorectal cancer: mutations in a signaling pathway. *Nature* **2005**, *436*, 792.
- (12) Vogt, P. K.; Bader, A. G.; Kang, S. PI3-kinase hidden potential revealed. *Cell Cycle* **2006**, *5*, 946–949.
- (13) Workman, P.; Clarke, P. A.; Guillard, S.; Raynaud, F. I. Drugging the PI3 kinome. *Nat. Biotechnol.* **2006**, *24*, 794–796.
- (14) Fan, Q. W.; Knight, Z. A.; Goldenberg, D. D.; Yu, W.; Mostov, K. E.; Stokoe, D.; Shokat, K. M.; Weiss, W. A. A dual PI3 kinase/mTOR inhibitor reveals emergent efficacy in glioma. *Cancer Cell* **2006**, *9*, 341–349.
- (15) Vlahos, C. J.; Matter, W. F.; Hui, K. Y.; Brown, R. F. A specific inhibitor of phosphatidylinositol-3-kinase, 2-(4-morpholinyl)-8-phenyl-4*H*-1-benzopyran-4-one (LY294002). *J. Biol. Chem.* **1994**, *269*, 5241–5248.
- (16) Yaguchi, S.; Fukui, Y.; Koshimizu, I.; Yoshimi, H.; Matsuno, T.; Gouda, H.; Hirono, S.; Yamazaki, K.; Yamori, T. Antitumor activity of ZSTK474, a new phosphatidylinositol-3-kinase inhibitor. *J. Natl. Cancer Inst.* **2006**, *98*, 545–556.
- (17) Kong, D.; Yamori, T. ZSTK474 is an ATP-competitive inhibitor of class I phosphatidylinositol-3-kinase isoform. *Cancer Sci.* **2007**, *98*, 1638–1642.
- (18) Folkes, A. J.; Ahmadi, K.; Alderto, W. K.; Alix, S.; Baker, S. J.; Box, G.; Chuckowree, I. S.; Clarke, P. A.; Depledge, P.; Eccles, S. A.; Friedman, L. S.; Hayes, A.; Hancox, T. C.; Kugendradas, A.; Lensun, L.; Moore, P.; Olivero, A. G.; Pang, J.; Patel, S.; Pergl-Wilson, G. H.; Raynaud, F. I.; Robson, A.; Saghir, N.; Salphati, L.; Sohal, S.; Ultsch, M. H.; Valenti, M.; Wallweber, H. J. A.; Wan, N. C.; Weismann, C.; Workman, P.; Zhyvoloup, A.; Zvebil, M. J.; Shuttleworth, S. J. The identification of 2-(1*H*-indazol-4-yl)-6-(4-methane sulfonyl-piperazin-1-ylmethyl)-4-morpholin-4-yl-thieno[3,2-*d*]pyrimidine (GDC-0941) as a potent, selective, orally bio-available inhibitor of class I PI3 kinase for the treatment of cancer. *J. Med. Chem.* **2008**, *51*, 5522–5532.
- (19) (a) Stauffer, F.; Maira, S. M.; Furet, P.; Garcia-Echeverria, C. Imidazo[4,5-*c*]quinolines as inhibitors of the PI3K/PKB-pathway. *Bioorg. Med. Chem. Lett.* **2008**, *18*, 1027–1030. (b) Maira, S. M.;

- Stauffer, F.; Brueggen, J.; Furet, P.; Schnell, C.; Fritsch, C.; Brachmann, S.; Chene, P.; De Pover, A.; Schemaker, K.; Fabbro, D.; Gabriel, D.; Simonen, M.; Murphy, L.; Finan, P.; Sellers, W.; Garcia-Echeverria, C. Identification and characterization of NVP-BEZ235, a new orally available dual phosphatidylinositol 3-kinase/mammalian target of rapamycin inhibitor with potent in vivo antitumor activity. *Mol. Cancer Ther.* **2008**, *7*, 1851–1863.
- (20) Garlich, J. R.; De, P.; Dey, N.; Su, J. D.; Peng, X.; Miller, A.; Murali, R.; Lu, Y.; Mills, G. B.; Kundra, V.; Shu, H.-K.; Peng, Q.; Durden, D. L. A vascular targeted pan phosphoinositide 3-kinase inhibitor prodrug, SF1126, with antitumor and antiangiogenic activity. *Cancer Res.* **2008**, *68*, 206–215.
- (21) (a) Zask, A.; Verheijen, J. C.; Curran, K.; Kaplan, J.; Richard, D. J.; Nowak, P.; Malwitz, D. J.; Brooijmans, N.; Bard, J.; Svenson, K.; Lucas, J.; Toral-Barza, L.; Zhang, W. G.; Hollander, I.; Gibbons, J. J.; Abraham, R. T.; Ayril-Kaloustian, S.; Mansour, T. S.; Yu, K. ATP-competitive inhibitors of the mammalian target of rapamycin: design and synthesis of highly potent and selective pyrazolopyrimidines. *J. Med. Chem.* **2009**, *52*, 5013–5016. (b) Zask, A.; Kaplan, J.; Verheijen, J. C.; Richard, D. J.; Curran, K.; Brooijmans, N.; Bennett, E. M.; Toral-Barza, L.; Hollander, I.; Ayril-Kaloustian, S.; Yu, K. Morpholine derivatives greatly enhance the selectivity of mammalian target of rapamycin (mTOR) inhibitors. *J. Med. Chem.* **2009**, *52*, 7942–7945. (c) Dehnhardt, C. M.; Venkatesan, A. M.; Chen, Z.; Delos Santos, E.; Dos Santos, O.; Bursavich, M.; Gilbert, A. M.; Ellingboe, J. W.; Ayril-Kaloustian, S.; Khafizova, G.; Brooijmans, N.; Mallon, R.; Hollander, I.; Feldberg, L.; Lucas, J.; Chaudhary, I.; Yu, K.; Gibbons, J.; Abraham, R.; Mansour, T. S. Lead optimization of N3 substituted-7-morpholino-triazolopyrimidines as dual phosphoinositide 3-kinase and mammalian target of rapamycin inhibitors: discovery of PKI-402. *J. Med. Chem.* **2010**, *53*, 798–810.
- (22) Yang, X.; Li, P.; Feldberg, L.; Kim, S. C.; Bowman, M.; Hollander, I.; Mallon, R.; Wolf, S. F. A directly labelled TR-FRET assay for monitoring phosphoinositide-3-kinase activity. *Comb. Chem. High Throughput Screening* **2006**, *9*, 565–570.
- (23) Toral-Barza, L.; Zhang, W. G.; Lamison, C.; Larocque, J.; Gibbons, J.; Yu, K. *Biochem. Biophys. Res. Commun.* **2005**, *332*, 304–310.
- (24) Yu, K.; Toral-Barza, L.; Discafani, C.; Zhang, W. G.; Skotnicki, J.; Frost, P.; Gibbons, J. *Endocr-Relat. Cancer* **2001**, *8*, 249–258.
- (25) Venkatesan, A. M.; Dehnhardt, C. M.; Chen, Z.; Delos Santos, E.; Dos Santos, O.; Bursavich, M.; Gilbert, A. M.; Ellingboe, J. W.; Ayril-Kaloustian, S.; Khafizova, G.; Brooijmans, N.; Mallon, R.; Hollander, I.; Feldberg, L.; Lucas, J.; Yu, K.; Gibbons, J.; Abraham, R.; Mansour, T. S. Novel Imidazolopyrimidines as dual PI3-kinase, mTOR inhibitors. *Bioorg. Med. Chem. Lett.* **2010**, *20*, 653–657.
- (26) Chen, Z.; Venkatesan, A. M.; Dehnhardt, C. M.; Ayril-Kaloustian, S.; Mansour, T. S.; Brooijmans, N.; Mallon, R.; Hollander, I.; Yu, K. Discovery of Novel Pyrrolo[3,2-*d*]pyrimidine Derivatives as PI3-Kinase Inhibitors. Presented at the 238th National Meeting of the American Chemical Society, Washington, D.C., August 16–20, **2009**.
- (27) Kaplan, E. L.; Meier, P. Nonparametric estimation from incomplete observations. *J. Am. Stat. Assoc.* **1958**, *53*, 457–481.